Efficiency enhancement in dye-sensitized solar cells irrespective of the electrolyte medium by nanostructured tri-layer TiO_2 photoanode

H. N. M. Sarangika, M. A. K. L. Dissanayake & G. K. R. Senadeera

Ionics
International Journal of Ionics The Science and Technology of Ionic Motion

ISSN 0947-7047

Ionics
DOI 10.1007/s11581-020-03620-7

Springer

Ionics
https://doi.org/10.1007/s11581-020-03620-7

ORIGINAL PAPER

Efficiency enhancement in dye-sensitized solar cells irrespective of the electrolyte medium by nanostructured tri-layer TiO_2 photoanode

H. N. M. Sarangika[1] · M. A. K. L. Dissanayake[2,3] · G. K. R. Senadeera[2,4]

Received: 16 February 2020 / Revised: 15 April 2020 / Accepted: 10 May 2020

Abstract
A nanostructured, tri-layer TiO_2 photoanode consisting of a rice grain–shaped (RG), electrospun TiO_2 sandwiched between two TiO_2 nanoparticle (NP) layers has been successfully used for the efficiency enhancement in dye-sensitized solar cells (DSSCs) with three different types of electrolytes. The three different types of electrolytes, liquid, gel, and solid, were prepared, and their solar cell performances were assessed in order to establish that the efficiency enhancement due to the tri-layer TiO_2 photoanode occurs irrespective of the electrolyte type. The solar cell parameters of DSSCs with this novel photoanode were compared with DSSCs fabricated using a conventional TiO_2 nanoparticle (NP) single-layer photoanode. The electrolytes used were (a) commercially available Solaronix Iodolyte Z-50 liquid electrolyte (LE); (b) gel electrolyte (GE) consisting of PEO, EC, PC, KI, Pr_4NI, and I_2; and (c) solid electrolyte (SE) consisting of PAN, EC, PC, LiI, Pr4NI, BMII, and I_2.. Substantial improvement of efficiency of solar cells with NP/RG/NP composite electrode could be obtained irrespective of the type of the electrolyte medium. For the cells with gel polymer electrolyte (GE) and the solid polymer electrolyte (SE), the efficiency enhancement is 26.9% and 21.5% respectively, while the efficiency enhancement for the liquid electrolyte–based cell is 19.4%. The short-circuit photocurrent density values showed a similar enhancement due to the composite TiO_2 photoanode. These findings suggest that the efficiency and the photocurrent are enhanced considerably by the tri-layered photoanode structure evidently due to the improved light absorption by scattering events in the TiO_2 tri-layer.

Keywords Composite tri-layer TiO_2 photoanode · Dye-sensitized solar cells · Liquid electrolyte · Gel polymer electrolyte · Solid polymer electrolyte

Introduction

In DSSCs, electricity is generated at the semiconductor film on which a monolayer of visible light absorbing dye is attached. Photo-excitation of the absorbed dye molecule generates excited electrons which are injected into the conduction band of the semiconductor and quickly migrated to the external circuit through the conductive substrate. Therefore, the core component of the system is the semiconductor, which provides numerous adsorption sites for the dye sensitizer and functions as an electron accepter and electronic conductor [1]. TiO_2 is the most promising candidate for the DSSC photoanodes, because it possesses several favorable unique physical and chemical properties.

The primary role of the porous electrode is to provide a sufficient surface area for dye absorption, and to convey all injected electrons by the dye to the transparent conducting surface where the porous electrode is fabricated (TCO). A large internal surface area is the most essential requirement of the photoelectrode film in DSSCs, so that sufficient dye molecules can be adsorbed. Nanoporous materials satisfy this requirement by the formation of a porous interconnected network in which the

✉ H. N. M. Sarangika
sarangikah@appsc.sab.ac.lk

[1] Department of Physical Sciences and Technology, Sabaragamuwa University of Sri Lanka, Belihuloya, Sri Lanka

[2] National Institute of Fundamental Studies, Hanthana Road, Kandy, Sri Lanka

[3] Postgaduate Institute of Science, University of Peradeniya, Peradeniya, Sri Lanka

[4] Department of Physics, The Open University of Sri Lanka, Nawala, Nugegoda, Sri Lanka

Published online: 22 May 2020

specific surface area may be increased by more than 1000 times when compared with bulk materials.

A photoanode constructed conventionally with a nanoporous TiO_2 layer has several drawbacks. High porosity and proper pore sizes of the TiO_2 layer are essential for the enhanced dye absorption capacity and light scattering ability. However, the porous nature of the TiO_2 layer could leave some portions of a bare TCO-conducting surface uncovered with TiO_2 [2]. The redox electrolyte solution can then penetrate a porous structure to reach uncovered areas of the TCO conduction surface. The direct exposure of the TCO to the redox electrolyte permits electrochemical reduction of I_3^- at the interface with the photogenerated electron. This process is equivalent to the direct recombination of the photoelectron with an excited dye molecule. As a result of this, a drastic reduction in photocurrent and energy conversion efficiency can occur [3].

A highly porous TiO_2 layer might also lead to insufficient connectivity between TiO_2 nanoparticles. This is another drawback of the nanoporous photoanode. Non-interconnected particles will result in a limited number of effective electron pathways. Lack of pathway for electron migration would lead to a higher resistance and a larger probability of electron recombination. Therefore, photoelectron recombination is intensified by the decrease in interconnectivity and increase in electron transfer resistance [4].

Although TiO_2 nanoparticles have sufficient surface area for the attachment of dye molecules, structural disorder leads to scattering of free electrons and a reduction in carrier mobility [5]. To overcome this drawback, one-dimensional nanostructures including TiO_2 nanowires, nanorods, nanotubes, and their composites with TiO_2 nanoparticles have been studied [5, 6]. However, insufficient dye molecule attachment by these one-dimensional structures is another challenge. Transmission of incident light with wavelengths longer than 600 nm through the nanoporous TiO_2 photoanode would reduce solar light harvesting. Therefore, additional scattering layers need to be developed on to the photoanode to improve the light absorbance [7]. In this approach, photoanode materials with various morphologies such as nanoparticles [1, 7], ordered meso-structured materials, and one-dimensional structured materials (nanorod, nanowire and nanotube) [8, 9], have been widely studied. In the recent past, several methods such as sol–gel, hydrothermal processes, electrochemical anodization, electrospinning, electrospray, electrodeposition, directional chemical oxidation, chemical vapor deposition, and laser pyrolysis have been developed to prepare the TiO_2 nanostructures with controllable size, morphology, and uniformity [10]. Among the available methods mentioned above, electrospinning is a simple and versatile nanofabrication technique. It can prepare several continuous 1D nanofibers of polymers, ceramics, composites, and metals with controllable diameter ranging from a few nanometers to several micrometers. In 2003, the first discovery of electrospun TiO_2 nanofibers was reported and thereafter many studies have been performed using electrospun TiO_2 nanofibers in photovoltaic devices [10, 11].

In order to gain a high surface-to-volume ratio and light scattering layer, a bilayer TiO_2 nanofiber photoanode was prepared by both small- and large-diameter nanofibers [12] and use of this photoanode could obtain efficiency enhancement from 7.14 to 8.40%. Joshi et al. [5] reported that the composite made of electrospun TiO_2 nanofibers and conventional TiO_2 nanoparticle noticeably improves the harvesting of light. Hu et al. [13] also reported that the maximum efficiency of the DSSCs fabricated with highly porous nanofibers produced by electro-spinning is significantly higher than that of DSSCs made with non-porous TiO_2 nanofibers. By considering the above facts in this study, an innovative type of TiO_2 composite photoanode consisting of a rice grain–shaped TiO_2 nanostructure (RG) layer sandwiched between two TiO_2 nanoparticle (NP) layers (NP/RG/NP) has been fabricated and tested in dye-sensitized solar cells using three different types of electrolytes. Previously reported studies on dye-sensitized solar cells made with rice grain–shaped and other TiO_2 nanostructured photoanodes are based on liquid electrolytes [14, 15]. This is the first study comparing the performance of the DSSCs based on a single-TiO_2-nanoparticle photoanode and a composite TiO_2-tri-layer photoanode (NP/RG/NP) fabricated with three different types of redox electrolytes, liquid, gel, and solid.

Materials and methods

Electrode preparation and characterization

In order to obtain a nanoparticle layer of TiO_2 (NP), commercially available TiO_2 nanoparticle paste (Solaronix D) was coated on a pre-cleaned fluorine-doped tin oxide conducting glass (FTO, sheet resistance 12 Ω/sq) by the doctor blade technique and sintered at 250 °C for 30 min, 1.5 g poly (vinyl acetate) (PVA, Mw = 140,000) (Aldrich), 3 g titanium(IV) isopropoxide (TiP) (Aldrich), and 1.2 g of acetic acid as a catalyst for sol–gel reaction in 19 ml of N,N-dimethylformamide (DMF) (Fluka) were mixed together under magnetic stirring for 4 h. TiO_2 nanofibers were electrospun directly onto a nanoparticle layer under an applied voltage of 15 kV with a solution injection rate of 2 ml/h by using the prepared mixture. An FTO substrate with the above nanoparticle layer was kept at a distance of 7 cm below the needle of the electrospinning unit. After electrospinning, a TiO_2 web was kept in an air for 1 h prior to calcinations. The calcination was carried out stepwise at each temperature as 100 °C (15 min), 150 °C (15 min), 325 °C (5 min), and 450 °C (1 h) in air. After that, commercially available TiO_2

paste was coated on the fiber mat by the doctor blade technique and sintered at 450 °C for 45 min. Morphology of the fibers with a rice grain shape (RG) was confirmed by taking scanning electron micrograph (SEM) images of the electrodes. The above sintered TiO_2 films were then dipped in an ethanolic dye solution containing 0.3 mM of ruthenium dye (N719, Solaronix) at room temperature for 72 h.

Electrolytes used

In order to check the dependence of the performance of DSSCs on the electrolyte medium, three different types of electrolyte compositions were prepared: (a) commercially available Solaronix Iodolyte Z-50 liquid electrolyte (LE), (b) gel electrolyte (GE) consisting of PEO, EC, PC, KI, Pr_4NI (tetrapropylammonium iodide), and I_2, and (c) solid electrolyte (SE) consisting of PAN, EC, PC, LiI, Pr_4NI, BMII (1-butyl-3-methylimidazolium iodide), and I_2. The following tables show the electrolyte composition with their percentage.

Dye-sensitized solar cell fabrication and characterization

DSSCs were prepared by sandwiching the electrolytes between the dye-sensitized NP/RG/NP TiO_2 working electrode and the platinum counter electrode with the configuration of glass/FTO/TiO_2/dye/electrolyte/Pt/. DSSCs with conventional NP photoanode were also prepared for comparison. Fabricated solar cells were irradiated with light of 1000 W cm^{-2} with an AM 1.5 air mass filter (Newport Oriel LCS-100 solar simulator) and I–V characteristics were obtained using a Metrohm Autolab PGSTAT128N with FRA32 frequency module.

Dye absorption of the NP electrode and NP/RG/NP electrode was estimated by using the following method. Areas (0.25 cm^2) of prepared electrodes were soaked in ethanolic dye solution containing 0.3 mM of ruthenium dye (N719, Solaronix) at room temperature for 72 h to complete sensitizer loading. Then, the electrodes were sequentially washed with water/ethanol and dried in the air. In order to analyze the loading amount of the dye in the TiO_2 electrode, the dye was desorbed from the TiO_2 electrode into the diluted NH_3 solution. The dye absorbance was measured by a Shimadzu 2450 UV-vis spectrophotometer.

Electrochemical impedance spectroscopy (EIS) measurements were performed under light condition on DSSCs using the Metrohm Autolab Potentiostat/Galvanostat PGSTAT 128 N coupled to a FRA 32 M frequency response analyzer (FRA) covering the 1-MHz to 1-mHz frequency range and using the AC voltage signal of 10 mV. Impedance plots as well as plots of phase angle vs frequency (bode phase) were analyzed in order to find the electron recombination lifetime.

Results and discussion

Morphology of the electrospun, rice grain–shaped TiO2 nanostructure

Figure 1 shows the SEM image of the electrode after sintering at 450 °C. This SEM image confirms the rice grain–shaped TiO_2 nanostructure. The average dimensions of the nanostructures were 260 nm length and 70 nm diameter. The shape of the nanostructure has two sharp ends and is well matched with the typical rice grain. The electrospun TiO_2 nanofibers did not show any rice grain–shaped structures, but the sintered sample showed a rice grain–shaped structure. The origin of this unique rice grain–shaped nanostructure can be traced to the microscale phase separation between TiO_2 and the polymer during solvent evaporation owing to the solubility difference between the two. This could lead to the breaking up of the continued TiO_2 fibers into short structures as confirmed by Shengyuan et al. [11]. It is clearly seen that the TiO_2 rice grains have an elongated bead-type, rice grain–shaped nanostructure that appears to be favorable for enhancing the light scattering ability [16].

I–V characteristics of DSSC with three different electrolyte phases: liquid, gel, and solid electrolytes

Characterization of solar cells fabricated using three different electrolytes described above were done using the cell configuration FTO/TiO_2/dye/electrolyte/Pt/FTO. Current-voltage characteristic curves of the DSSCs were fabricated using the three different types of electrolytes: (a) commercially available Solaronix Iodolyte Z-50 liquid electrolyte (LE), (b) gel polymer electrolyte (GE), and (c) solid polymer electrolyte (SE) and NP/RG/NP composite electrode, are shown in Fig. 2. I–V characteristics of dye-sensitized solar cells fabricated using the same electrolytes and conventional NP TiO_2

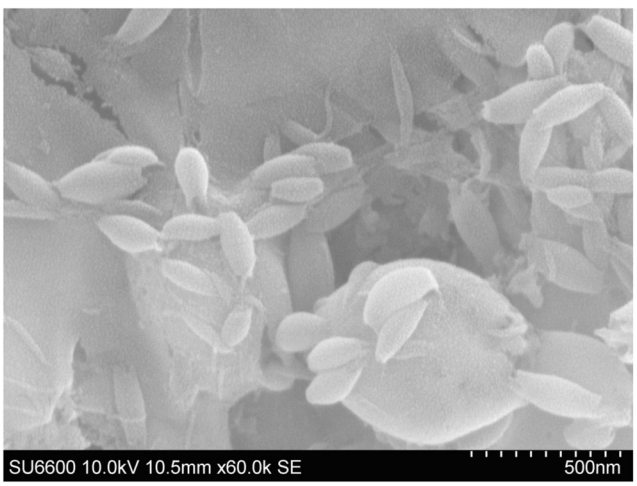

Fig. 1 SEM images of the sintered rice grain-shaped TiO_2 nanostructure

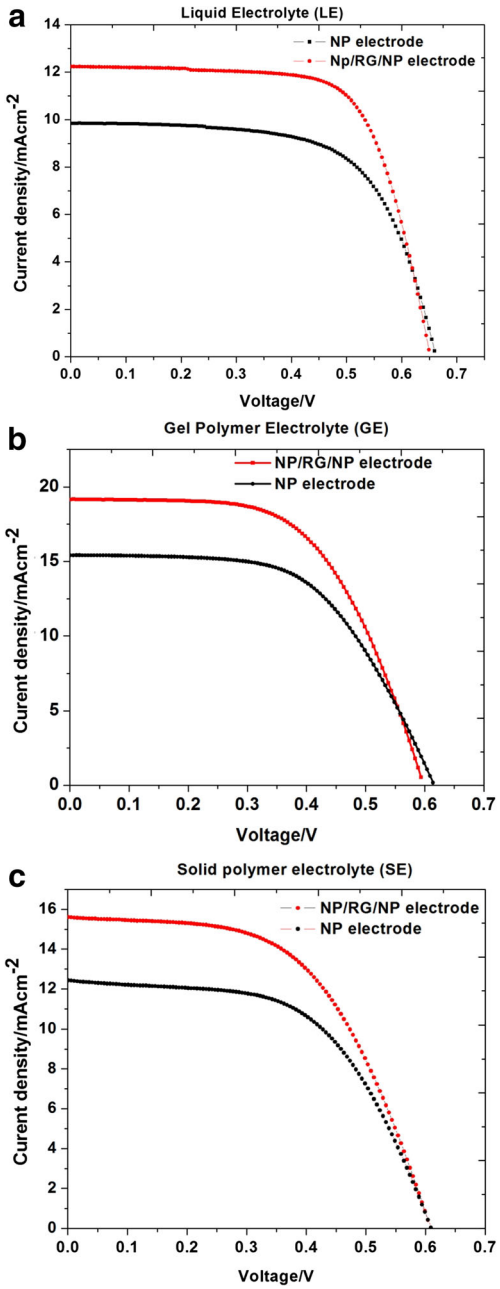

Fig. 2 Photocurrent–photovoltage (I–V) characteristic curves for solar cell with configuration FTO/TiO_2/dye/electrolyte/Pt/FTO fabricated with different electrolyte compositions. **a** Liquid electrolyte (LE). **b** Gel polymer electrolyte (GE). **c** Solid polymer electrolyte (SE)

photoanode are also shown in Fig. 2. Table 2 summarizes the photovoltaic parameters obtained from Fig. 2. The fill factor (FF) and the efficiency (η%) were calculated using the open-circuit voltage (V_{oc}) and the short-circuit current density (J_{sc}) using the relationships in Eqs. 1 and 2.

$$\mathrm{FF} = \frac{I_{opt} V_{opt}}{j_{sc} V_{oc}} \tag{1}$$

The fill factor is calculated by dividing the product of current (I_{opt}) and voltage (V_{opt}) measured at the power point (maximum output power P_{max}) by the product of short-circuit current and the open-circuit voltage. The power point is the maximum product of the cell voltage and photocurrent obtained on the I–V curve.

$$\eta = \frac{J_{sc} V_{oc} \mathrm{FF}}{P_{in}} \tag{2}$$

It can be seen that the current density and the efficiency have significantly enhanced for the DSSC with the composite tri-layer photoanode NP/RG/NP irrespective of the electrolyte medium compared with the control cells with a single TiO_2 layer NP photoanode with equal thickness. It is interesting to study the reason for this efficiency enhancement. The presence of the TiO_2 elongated "bead-like" network structure formed from the TiO_2 nanofiber layer after sintering affects the specific surface area, porosity, light scattering, and electron transport rate in the TiO_2 composite photoanode. Efficiency enhancement for the liquid, gel, and solid electrolyte–based DSSCs with a tri-layer photoanode compared with the DSSCs with single-TiO_2-layer photoanodes are 20%, 27%, and 21%, respectively. According to I–V curves shown in Fig. 2, the efficiency enhancement in all three types of DSSCs is essentially due to the increase in the photocurrent. It should be mentioned here that due the different nature of the (solvent type, composition, etc.) different liquid electrolytes used for the fabrication of DSSCs (Table 1), it is difficult to compare the current densities and efficiencies of three DSSCs based on LE, GE, and SE electrolytes made with a single-layer (TP) photoanode. The same is true for the DSSCs based on LE, GE, and SE electrolytes made with a tri-layer NP/NF/NP electrode. This is because their conductivities, viscosity-dependent ionic mobilities, and diffusion/penetration of the electrolyes into the photoanode structure are different. However, for a given electrolyte type, we can clearly compare the performance between the two DSSCs, one with a single-layer NP photoanode and the other DSSC with the tri-layer NP/NF/NP photoanode. Such a comparison clearly demonstrates that the photocurrent density and the efficiency of the DSSCs made with the triple-layer NP/NF/NP photoanode have significantly enhanced compared with the DSSC made with a single-NP-layer photoanode. It is very likely that the enhanced photocurrents in the triple-layer photoanode-based cells is due to the increased light absorption by the tri-layer nanostructure due to the multiple scattering events within the "rice grain"–shaped nanostructure of the TiO_2 nanofibers. This is in agreement with the explanation given in relation to a related study on TiO_2-tri-layer photoanode-based DSSCs [15].

Table 1 Three different electrolyte compositions

Electrolyte	Composition						
(a) Liquid electrolyte (LE)	Commercially available liquid electrolyte: Solaronix Iodolyte Z-50						
(b) Gel polymer electrolyte (GE)	EC wt%	PC wt%	PEO wt%	KI wt%	Pr4NI wt%	I_2 wt%	
	35.97	35.97	11.99	7.19	7.19	1.68	
(c) Solid polymer electrolyte (SE)	EC wt%	PC wt%	PAN wt%	LiI wt%	Pr4NI wt%	I_2 wt%	BMII wt%
	40.93	37.97	9.86	4.35	4.37	1.28	1.24

Dye adsorption by two different photoanodes: NP photoanode and NP/RG/NP composite photo anode

In order to check whether the observed efficiency enhancement is resulting from the enhanced dye adsorption or not by the tri-layer electrode, dye adsorption for each of these electrodes were measured. Figure 3 shows the dye adsorption of these two types of electrodes: conventional NP electrode and NP/RG/NP composite electrode. It can be clearly seen that there is no significant difference in dye adsorption between these two types of electrodes. Therefore, we can assume that this efficiency enhancement originates from a different mechanism which is very likely be the enhanced light absorption by the three-layer composite photoanode.

Electrochemical impedance spectroscopic analysis

EIS measurements were taken to investigate the electron transport properties of the DSSCs with these two types of electrodes. Nyquist plots of the electrochemical impedance spectra shown in Fig. 4 were taken in the frequency range from 1.0 mHz to 1×10^6 Hz. Each Nyquist plot exhibits three semicircles as expected. The small semicircle in the high-frequency range is assigned to the charge transfer resistance (R_{1CT}) at the redox electrolyte/Pt counter electrode interface. The second semicircle in the mid frequency region is attributed to the transport of injected electrons within the TiO_2 film and the charge transfer across the TiO_2/redox electrolyte interface. The third semicircle in the low-frequency region is attributed to the Nernst diffusion within the electrolyte. Figure 4 shows the Nyquist plots of the electrochemical impedance spectra of DSSCs made with two different types of electrodes (TiO_2 single-layer NP and triple-layer NP/RG/NP) with three different redox electrolytes, namely, liquid electrolyte (LE), gel polymer electrolyte (GE), and solid polymer electrolyte (SE).

The impedance parameters were extracted by using the equivalent circuit model, and values of the charge transfer resistance of TiO_2/electrolyte interface (R_{2CT}) for the DSSCs fabricated with three different electrolytes are summarized in Table 3. Impedance parameters taken for DSSCs made with the conventional single-layer NP electrode are also shown in the Fig. 4 and Table 3 for comparison. From the data given in Table 3, one can clearly see that DSSCs fabricated with the composite NP/RG/NP tri-layer electrodes with a rice grain–shaped TiO_2 RG nanostructure exhibit lower R_{2CT} values for all three types of electrolytes, implying a more efficient charge transfer process across the TiO_2/electrolyte interface, compared with the single-layer TiO_2 nanoparticle (NP) electrode which shows a higher R_{2CT} value. This trend is maintained by all DSSCs irrespective of the nature of the redox electrolyte medium, proving that the newly prepared tri-layer NP/RG/NP photoanode poses much better electron transport properties within the composite tri-layer TiO_2 photoanode and across the photoanode/electrolyte interface, compared with the DSSCs made with a single-layer TiO_2 NP layer photoanode. Similar observations have been reported by other groups [17–21].

When the impedance data are represented as plots of phase angle vs frequency (Bode plots), characteristic frequency

Table 2 Parameters of the solar cells fabricated with three different electrolyte types

Type of the electrolyte used	Electrode configuration	J_{sc} (mA cm^{-2})	V_{OC} (mV)	FF%	Efficiency η%
Liquid electrolyte (a) (LE)	NP electrode	11.12	650	70.4	5.06
	NP/NF/NP composite electrode	14.53	639	65.4	6.04
Gel electrolyte (b) (GE)	NP electrode	15.41	614	57.9	5.45
	NP/NF/NP composite electrode	19.16	604	59.8	6.92
Solid electrolyte (c) (SE)	NP electrode	12.42	609	56.5	4.24
	NP/NF/NP composite electrode	15.60	604	55.6	5.15

Table 3 Charge transfer resistance of TiO_2/electrolyte interface (R_{2CT}), current density (J_{SC}), and recombination electron life time (τ) for the DSSCs fabricated with TiO_2 NP electrode, TiO_2 NP/RG/NP tri-layer electrode, and three different electrolyte media, liquid electrolyte (LE), gel polymer electrolyte (GE), and solid polymer electrolyte (SE)

	TiO_2 NP electrode			TiO_2 NP/RG/NP tri-layer electrode		
	LE	GE	SE	LE	GE	SE
R_{2CT} (Ω)	11.2	5.82	17.1	9.28	5.39	13.5
J_{SC} (mA cm^{-2})	11.12	15.41	12.42	14.53	19.16	15.6
Efficiency (η%)	5.06	5.45	4.24	6.04	6.92	5.15
Electron lifetime (τ/ms)	6.3	10.1	18.0	7.9	18.1	29.4

peaks for cells fabricated with NP electrode have shifted to the high-frequency region compared with cells fabricated with the NP/RG/NP electrode as shown in Fig. 5. This characteristic frequency is related to the inverse of the recombination life time (τ) of the electrons in the TiO_2 film. The following equation defines the recombination life time in TiO_2-based DSSCs.

$$\tau = \frac{1}{\omega_{\min}} = \frac{1}{2\pi f_{\max}} \tag{3}$$

where $\omega_{\min} = 2\pi f_{\max}$ and $f_{\max}$ is the peak frequency.

Therefore, the electron lifetime τ for the DSSCs fabricated with TiO_2NP/RG/NP tri-layer composite electrode shows a higher value compared with the value for the DSSCs fabricated with the TiO_2NP single-layer electrode. As shown in Table 3, this result is true for the DSSCs made with the three different types of the electrolyte medium. As revealed from Table 3 and Fig. 5, the TiO_2NP/RG/NP tri-layer nanostructure with rice grain–shaped TiO_2 nanofibers has significantly increased the electron lifetimes making the photogenerated electrons to remain for a longer time without undergoing recombination. This suggests that electrons within the tri-layer photoanode are efficiently transferred resulting in a higher

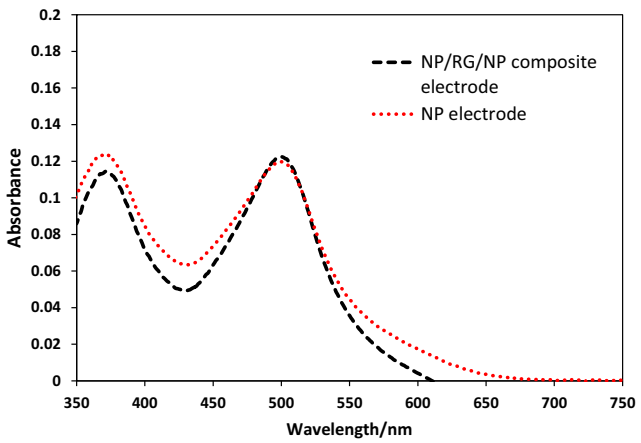

Fig. 3 Absorption of aqueous dye solutions (Solaronix) after desorption from TiO_2 photoanode

J_{SC} and higher energy conversion efficiency compared with the DSSC made with a single TiO_2 NP layer photoanode. This result is also true irrespective of the nature of the redox electrolyte. Similar results have been reported for nanocrystal/nanotube double-layered films with liquid electrolyte composed of 1.0 M 2,3-dimethyl-1-propylimidazolium iodide, 0.12 M I_2, 0.1 M LiI, and 0.5 M tert-butylpyridine in 3-methoxypropionitrile [22] and for PbS/Hg quantum dot-sensitized, highly efficient solar cell structures with triple-layered TiO_2 photoanode [17].

DSSCs fabricated with NP + RG and NP + NF composite TiO_2 electrodes have also been reported with a two-layered structure [23] with liquid electrolyte and showed 15.5% efficiency enhancement. In comparison, the present study using a tri-layer NP/RG/NP TiO_2 photoanode has gained efficiency enhancements of 19.36%, 26.97%, and 21.46% respectively for the liquid electrolyte (LE), gel polymer electrolyte (GE), and solid polymer electrolyte (GE)–based solar cells, which is a novel finding not reported in previous studies. Koo et al. [24] reported nano-embossed hollow spherical TiO_2 (NeHS TiO_2) for use in high-efficiency DSSCs. After NeHS TiO_2 is introduced as an overlayer, the conversion efficiency is improved by 21%. This result is comparable with results obtained by us for the liquid electrolyte–based cells. However, conversion efficiency enhancement of 26.97% and 21.46% for gel polymer electrolyte and solid polymer electrolyte is important. Since most of the efficient DSSCs consist of liquid-type electrolytes, their practical applications are limited due to some technological problems, such as durability, liquid leakage, and relatively poor long-term stability generally associated with some chemical constituents of these electrolytes. Therefore, the gel and solid electrolyte–based DSSCs developed by us in this work should be able to improve the long-term operational stability of these solar cells.

Incident photon to current conversion efficiency measurements

Figure 6 shows the incident-photon to current conversion efficiency (IPCE) as a function of wavelength for two electrodes

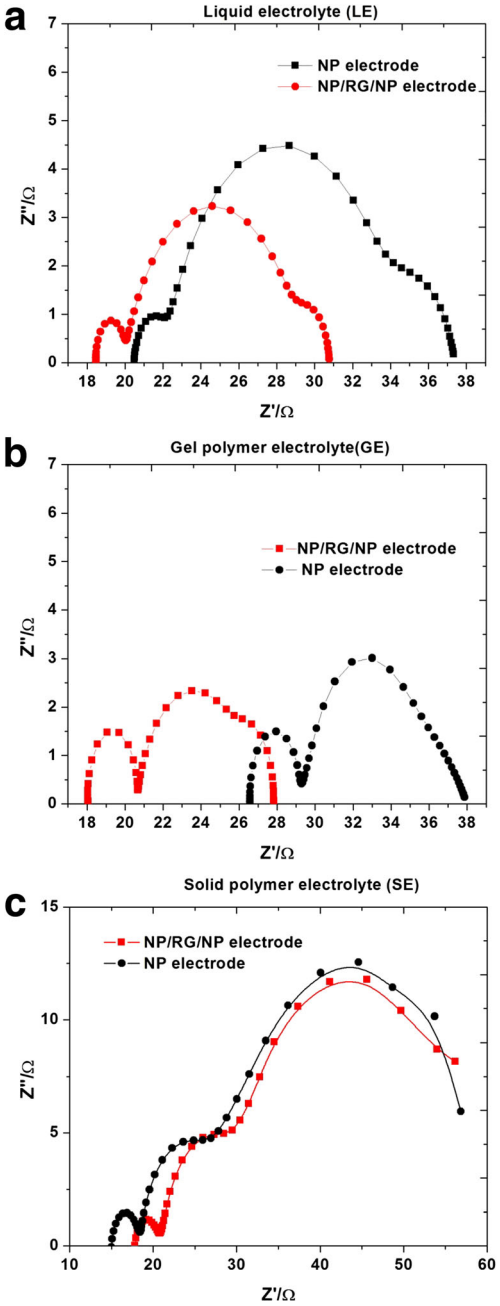

Fig. 4 Nyquist plots of the DSSCs with configuration FTO/TiO_2/dye/electrolyte/Pt/FTO made with the three different electrolyte media. **a** Liquid electrolyte (LE). **b** Gel polymer electrolyte (GE). **c** Solid polymer electrolyte (SE)

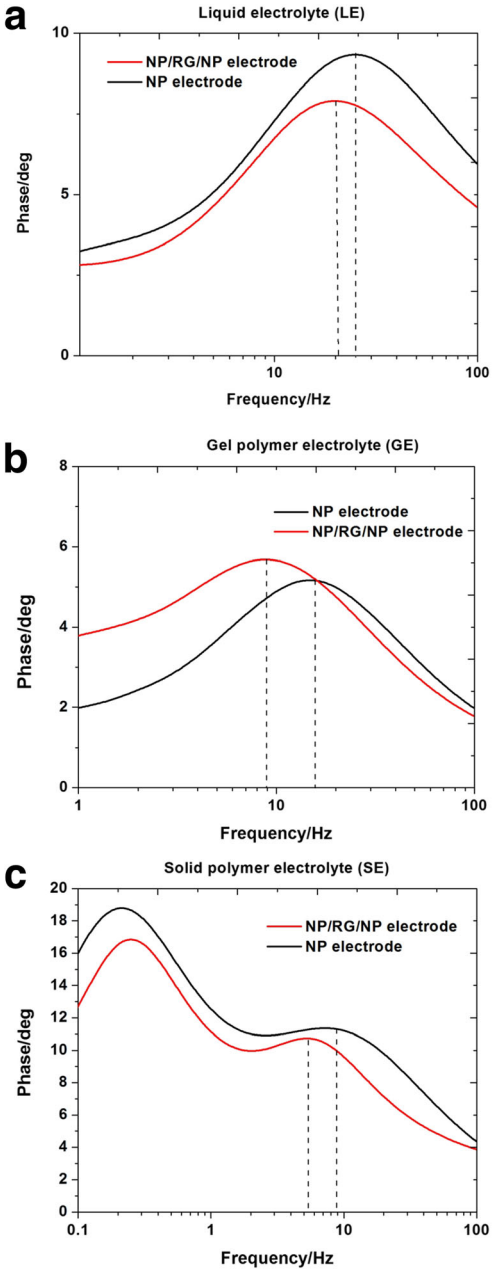

Fig. 5 Impedance data plotted as phase angle vs frequency (Bode plots) for the DSSCs fabricated with NP electrode and NP/RG/NP composite electrode with three different electrolyte types. **a** Liquid electrolyte (LE). **b** Gel polymer electrolyte (GE). **c** Solid polymer electrolyte (SE)

with PEO-based gel polymer electrolyte (GE). The absolute IPCE of the NP/RG/NP electrode is higher than that of the NP electrode over the entire wavelength region. This is in good agreement with observed higher photocurrent current density. Higher IPCE in the visible and longer-wavelength regions implies that a large part of the light incident on DSSCs can be effectively "trapped" by the NP/RG/NP electrode through multiple scattering events and generate more photoexcited electrons [15].

In a study to compare the performance of DSSCs made with P25 TiO_2 photoanode with a nitrogen (N)-doped TiO_2 photoanode, Dissanayake et al. have observed that the charge transfer resistance of the TiO_2/electrolyte interface ($R2_{CT}$) of the N-doped TiO_2-based DSSCs was lower than the P25 TiO_2-based DSSCs [17]. Correspondingly, the J_{SC} values and the efficiencies of the DSSCs with N-doped TiO_2 photoanode have increased compared with DSSCs made with undoped P25 TiO_2 photoanode. This has been attributed to the change in the surface properties of the TiO_2 film due to

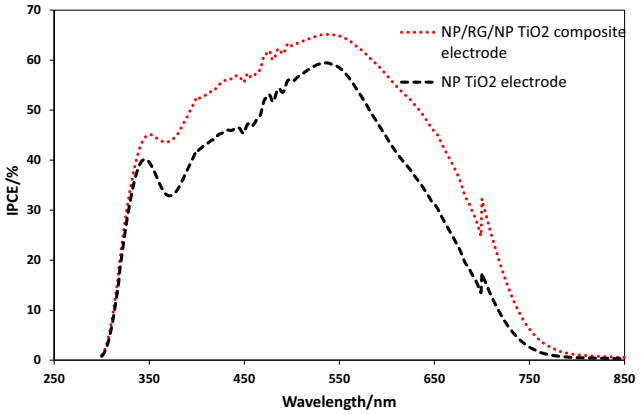

Fig. 6 IPCE spectra of DSSCs based on NP electrode and NP/RG/NP composite electrode with gel polymer electrolyte (GE)

nitrogen doping which improves the electron transfer mechanism at the N-TiO_2/electrolyte interface.

Based on a study of DSSCs made with the TiO_2 composite tri-layer nanorod/nanotube/nanorod (NR/NT/NR) photoanode, Zhangkai et al. have confirmed that the DSSCs with tri-layer photoanode have significantly enhanced photocurrent density and efficiency compared with the DSSCs made with a single TiO_2-layer photoanode [18]. This has been attributed to an increase in photocurrent density due to the increase in light absorption by the tri-layer photoanode structure. The slightly reduced open-circuit voltage was associated with the lower charge transfer resistance R_{2CT} at the TiO_2/electrolyte interface compared with the DSSCs made with single-layer TiO_2 nanoparticle-based cells.

High-efficiency of DSSCs based on multi-layered TiO_2 composite photoanodes consisting of (a) nanoparticle/nanoparticle (NP/NP) bilayer and (b) nanoparticle/nanorod (NP/NR) bilayer have been compared by Wang et al. [19]. Higher photocurrent with higher efficiency was obtained for the DSSCs with TiO_2 NP/NR bilayer photodiode compared with the TiO_2 NP/NP photoanode. Compared with DSSCs with NP/NP bilayer photoanode, the DSSCs with NP/NR photoanode have exhibited a lower charge transfer resistance at the TiO_2/electrolyte interface, and lower charge recombination rate (or higher electron life time). Authors have attributed the increased photocurrent and efficiency to enhanced light absorption by scattering effect in the NP/NR photoanode, compared with the NP/NP photoanode. Lanfang et al. [20] have used crystalline 3.6 nm TiO_2 quantum dots (QDs) well to fabricate blocking under layers in dye-sensitized solar cells to suppress the dark currents. Power conversion efficiency has been enhanced from 7.10 to 9.43% which has been attributed to the increase in electron life time and the decrease in charge transfer resistance at the dye-coated TiO_2/electrolyte interface.

Our TiO_2 NP/RG/NP three-layer sandwiched structure enables more efficient light trapping due to positioning of the two NP layers on either side of the middle scattering layer with a rice grain–shaped TiO_2 nanostructure. The main advantage of this novel three-layer design for the TiO_2 photoanode is that the light entering the photoanode can be utilized most efficiently due to the multiple scattering effects by the elongated rice grain–shaped TiO_2 beads [15]. The middle layer with rice grain (RG)–shaped TiO_2 beads makes an impressive contribution through scattering for the efficient generation of photoelectrons by the sensitized dye molecules in the two NP layers as well. Based on published data, it is clear that it is difficult to separate out the competition between electron transportation and recombination from EIS data alone. In general, a higher R_{2CT} value would suppress the back electron recombination at the TiO_2/electrolyte interface and thereby increase the V_{OC}. However, in the present case, we see a drop in the V_{OC} value for the DSSC with tri-layer photoanode consistent with decreased R_{2CT} implying that surface states and oxygen vacancies are acting as recombination pathways, to decrease the V_{OC}. This process appears to compete with the much stronger process of photoelectron generation due to intense light absorption by the DSSC with NP/RG/NP tri-layer TiO_2-nanostructured photoanode and corresponding increase in J_{SC} compared with the DSSC with a single TiO_2 NP layer.

Conclusions

We have prepared the "rice grain" (RG)–shaped TiO_2 nanostructure using the electrospinning method and investigated their photovoltaic property in dye-sensitized solar cells with three different types of electrolytes in three different phases: liquid, gel, and solid. DSSCs were fabricated with conventional NP electrode, and the results were compared with NP/RG/NP electrode. The SEM images confirm that the TiO_2 structure has an elongated bead like rice grain–shaped TiO_2 nanostructure. Though there is no significant difference in dye adsorption by these two electrodes, substantial improvement of efficiency for the NP/RG/NP composite electrode has been obtained irrespective of the electrolyte medium. The major contribution to the efficiency enhancement appears to come from the improved J_{SC}. This has been attributed to enhanced light absorption due to multiple scattering events by the TiO_2 rice grain shaped nanofibers within the TiO_2 tri-layer nanostructure. This is associated with reduced charge transfer resistance between the TiO_2 photoanode and electrolyte interface and the increased electron lifetime.

References

1. Grätzel M (2003) Dye-sensitized solar cells. J Photochem Photobiol C Photochem Rev 4:145–153

2. Zhang J, Zaban A (2008) Efficiency enhancement in dye-sensitized solar cells by in situ passivation of the sensitized nanoporous electrode with Li2CO3. Electrochim Acta 53:5670–5674
3. Diamant Y, Chappel S, Chen S, Melamed O, Zaban A (2004) Core–shell nanoporous electrode for dye sensitized solar cells: the effect of shell characteristics on the electronic properties of the electrode. Coord Chem Rev 248:1271–1276
4. Kopidakis N, Benkstein KD, van de Lagemaat J, Frank AJ (2003) Transport-limited recombination of photocarriers in dye-sensitized nanocrystalline TiO_2 solar cells. J Phys Chem B 107:11307–11315
5. Joshi P, Zhang L, Davoux D, Zhu Z, Galipeau D, Fong H, Qiao Q (2010) Composite of TiO_2 nanofibers and nanoparticles for dye-sensitized solar cells with significantly improved efficiency. Energy Environ Sci 3:1507–1510
6. Lanfang Q, Zhang L, Wu W, Wu J, Jianming L, Miaoliang H (2014) High-efficiency dye-sensitized solar cells based on ultra-long single crystalline titanium dioxide nanowires. J Power Sources 266:440–447
7. Canever N, Hughson F, Macdonald TJ, Nann T (2017) Electrospinning of photocatalytic electrodes for dye-sensitized solar cells. J Vis Exp 124:e55309
8. Shankar K, Bandara J, Paulose M, Wietasch H, Varghese OK, Mor GK, LaTempa TJ, Thelakkat M, Grimes CA (2008) Highly efficient solar cells using TiO_2 nanotube arrays sensitized with a donor-antenna dye. Nano Lett 8:1654–1659
9. Senadeera G, Kobayashi S, Kitamura T, Wada Y, Yanagida S (2005) Versatile preparation method for mesoporous TiO_2 electrodes suitable for solid-state dye sensitized photocells. Bull Mater Sci 28:635–641
10. Frenot A, Chronakis IS (2003) Polymer nanofibers assembled by electrospinning. Curr Opin Colloid Interface Sci 8:64–75
11. Shengyuan Y, Peining Z, Nair AS, Ramakrishna S (2011) Rice grain-shaped TiO_2 mesostructures—synthesis, characterization and applications in dye-sensitized solar cells and photocatalysis. J Mater Chem 21:6541–6548
12. Yang L, Leung WWF (2011) Application of a bilayer TiO_2 nanofiber photoanode for optimization of dye-sensitized solar cells. Adv Mater 23:4559–4562
13. Jung WH, Kwak NS, Hwang TS, Yi KB (2012) Preparation of highly porous TiO_2 nanofibers for dye-sensitized solar cells (DSSCs) by electro-spinning. Appl Surf Sci 261:343–352
14. Dissanayake MAKL, Sarangika HNM, Senadeera GKR, Divarathna HKDWMNR, Ekanayake EMPC (2017) Application of a nanostructured, tri-layer TiO_2 photoanode for efficiency enhancement in quasi-solid electrolyte-based dye-sensitized solar cells. J Appl Electrochem 47:1239–1249
15. Dissanayake MAKL, Divarathna HKDWMNR, Dissanayake CB, Senadeera GKR, Ekanayake PMPC, Thotawattage CA (2016) An innovative TiO_2 nanoparticle/nanofibre/nanoparticle, three layer composite photoanode for efficiency enhancement in dye-sensitized solar cells. J Photochem Photobiol A Chem 322:110–118
16. Hore S, Nitz P, Vetter C, Prahl C, Niggemann M, and Kern R (2005) Scattering spherical voids in nanocrystalline TiO_2–enhancement of efficiency in dye-sensitized solar cells. Chemical Communications 2011-1223
17. Dissanayake MAKL, Kumari JMKW, Senadeera GKR, Thotawatthage CA (2017) A novel multilayered photoelectrode with nitrogen doped TiO_2 for efficiency enhancement in dye sensitized solar cells. J Photochem Photobiol A Chem 349:63–72
18. He Z, Jing L, Wang WD, Wang J, Tianjin Z (2017) Enhanced photovoltaic performance of TiO_2 dye-sensitized solar cell based on one-dimensional composite photoanode. Int J Electrochem Sci 12(2017):8918–8928
19. Wang G, Wei X, Yu J (2015) High-efficiency dye-sensitized solar cells based on electrospun TiO_2 multi-layered composite film photoanodes. Energy 86:196–203
20. Que L, Lan Z, Wu W, Wu J, Lin J, Huang M (2014) Titanium dioxide quantum dots: magic materials for high performance underlayers inserted into dye sensitized solar cells. J Power Sources 268:670–676
21. Zhang L, Wu JH, Jian Ming L, MiaoLiang H (2014) $TiCl_4$ assisted formation of nano-TiO_2 secondary structure in photoactive electrodes for high efficiency dye-sensitized solar cells. Sci China Chem 57:888–894
22. Xu H, Tao X, Wang DT, Zheng YZ, Chen JF (2010) Enhanced efficiency in dye-sensitized solar cells based on TiO_2 nanocrystal/nanotube double-layered films. Electrochim Acta 55:2280–2285
23. Zhu P, Nair AS, Yang S, Peng S, Ramakrishna S (2011) Which is a superior material for scattering layer in dye-sensitized solar cells—electrospun rice grain-or nanofiber-shaped TiO_2? J Mater Chem 21:12210–12212
24. Koo HJ, Kim YJ, Lee YH, Lee WI, Kim K, Park NG (2008) Nano-embossed hollow spherical TiO_2 as bifunctional material for high-efficiency dye-sensitized solar cells. Adv Mater 20:195–199